Article ID: 1006-8775(2010) 03-0201-09

RETRIEVING ATMOSPHERIC SOUNDING PROFILES AROUND TYPHOON YUNNA USING INFRARED HYPERSPECTRAL MEASUREMENTS AIRS

HUANG Bing (黄 兵)[1, 2], LIU Jian-wen (刘建文)[2], BAI Jie (白 杰)[2], LI Yao-dong (李耀东)[2, 3], GAO Shou-ting (高守亭)[3]

(1. School of Physics, Peking University, Beijing 100006 China; 2. Aviation Institute of Air Force, Beijing 100085 China; 3. Institute of Atmospheric Sciences, Chinese Academy of Sciences, Beijing 100029 China)

Abstract: In this study, we derived atmospheric profiles of temperature, moisture, and ozone, along with surface emissivity, skin temperature, and surface pressure, from infrared-sounder radiances under clear sky (cloudless) condition. Clouds were detected objectively using the Atmospheric Infrared Sounder under a relatively low spatial resolution and cloud-mask information from the Moderate Resolution Imaging Spectroradiometer under a high horizontal resolution; this detection was conducted using space matching. Newton's nonlinear physical iterative solution technique is applied to the radiative transfer equation (RTE) to retrieve temperature profiles, relative humidity profiles, and surface variables simultaneously. This technique is carried out by using the results of an eigenvector regression retrieval as the background profile and using corresponding iterative forms for the weighting functions of temperature and water-vapor mixing ratio. The iterative forms are obtained by applying the variational principle to the RTE. We also compared the retrievals obtained with different types of observations. The results show that the retrieved atmospheric sounding profile has great superiority over other observations by accuracy and resolution. Retrieved profiles can be used to improve the initial conditions of numerical models and used in areas where conventional observations are sparse, such as plateaus, deserts, and seas.

Key words: infrared remote sensing; retrieval; atmospheric sounding profile; MODIS; AIRS

CLC number: P407 **Document code:** A **doi:** 10.3969/j.issn.1006-8775.2010.03.001

1 INTRODUCTION

Meteorologists all over the world have been making considerable efforts to use satellite observations to improve the initial conditions of numerical models and to understand weather system structure, making significant progress since Andersson and Pailleux[1], MiliJa[2] and Gao et al.[3, 4] For example, in European Center for Medium-Range Weather Forecasts (ECMWF), more than 87% of the assimilated data was satellite radiance data and their derived products; these assimilated data play a very important role in improving the initial conditions of numerical models and the quality of their forecasting products. Meteorologists have also made significant progress in retrieving temperature and humidity profiles and cloud variables from satellite radiance observations. NASA released its operationally retrieved temperature and humidity products using the Moderate Resolution Imaging Spectroradiometer (MODIS) (Guan et al.[5, 6]), while domestic researchers retrieved surface temperature products using MODIS data (Cui et al.[7]). Nonetheless, considerable efforts are required to improve the quality of retrieved cloud products because most severe weather systems are examined using cloud variables such as cloud fraction, cloud liquid water, and cloud ice water. Liu et al.[17] attempted to retrieve temperature and humidity profiles and cloud liquid water using NOAA-16 ATOVS

Received date: 2010-01-23; **revised date:** 2010-04-19

Foundation item: project of the Ministry of Sciences and Technology of the People's Republic of China (GYHY200706020); projects of National Natural Science Foundation of China ((40975034, 40505009); project of State Key Laboratory of Severe Weather (2008LASW-A01)

Biography: HUANG Bing, Ph.D., mainly studying ensemble forecasts and tropical cyclones.

E-mail for corresponding author: huangbi_h@sohu.com

Note: Beginning from V.14(1) 2008, *Journal of Tropical Meteorology* is indexed and abstracted in Science Citation Index Expanded and Journal Citation Reports/Science Edition.

radiance observations. These retrieved products were well consistent with their observations; however, since their research is not yet operational, the data are not available to others. Atmospheric ozone content, derived from the ATOVS and MODIS sound data, is used to study and monitor environmental changes (Li et al.[8]). Implementation of the EOS observation system enhances these studies. NASA released its MOD_07L2 operational products retrieved from MODIS and the Atmospheric Infrared Sounder (AIRS) on the AQUA satellite. These products include temperature and humidity profiles, ozone content profiles, surface temperature, surface pressure, and effective spectral emissivity. However, their horizontal resolution is only 45 km (nadir), and the vertical resolution is restricted to 26 layers owing to the incomplete usage of the AIRS sound data. Significant contributions have been made toward improving the horizontal and vertical resolutions of the retrieved profiles (Huang et al.[9, 10]). Domestic research has not achieved sufficient success in this regard because the AIRS sounding data are broadcast indirectly and thus difficult to obtain.

In this study, by spatially matching the high-resolution MODIS cloud detection products, we investigated the cloud detection of hyperspectral infrared measurements obtained from the AIRS sounding data (Guan et al.[5, 6]). Furthermore, we obtained analytical forms of the weighting function from radiative transfer equations using the first term of the variational principle for retrieved variables such as atmospheric temperature and humidity. The profiles retrieved with the eigenvector statistics method were used as the background profiles in the retrieval method. Further, Newton's iterative method, from nonlinear physics, is applied to the radiative transfer equation (RTE) to obtain atmospheric temperature, humidity profiles, surface temperature, and surface pressure. The horizontal resolution of these profile products was 13.5 km, and the vertical resolution was 101 layers. Retrieving error can be restricted to the level of operational application, and, as a result, these profiles can be used to understand the recycling of energy and water on the earth under different climatic conditions. These profiles, together with the radiance data, can be assimilated to improve the initial condition of numerical models and can be used as conventional observations in cases where conventional meteorological observations are insufficient. The incoming high-quality mesoscale information could make numerical models more reliable, thereby offering a new opportunity to improve the monitoring of temperature, moisture, and ozone distributions, and the changes occurring therein.

2 DATA AND METHODOLOGY

On August 12, 2004, a broad trough region existed from North China to the Russian Far East, and a weak ridge was present in front of the trough. A long-wave trough over Western Europe moved westward daily, until a pressure ridge at its front overlapped with another pressure ridge that moved from central Mongolia to the upstream end of the Yellow River in China. This deepened the meridional circulation in the middle and north of Asia. Then, a broad low-trough region from North China to the Russian Far East expanded southward and deepened further, which separated the joined pressure ridge into two loops—one in the east and the other in the west. This condition remained unchanged until the night of August 15, 2004. The precipitation brought by the typhoon Yunna helped combat a drought occurring in the southern reach of the Changjiang River and in a major part in the south of China. However, the typhoon-caused gale and the coinciding low-pressure circulation pattern affected the land and rainstorms accompanying the typhoon severely damaged the Zhejiang province. Furthermore, floods, landslides, and mud-rock flows led to casualties and property loss in the Jiangxi, Anhui, Hubei, Jiangsu, and Henan provinces (Xu et al.[11]).

The main sounding instruments on Earth Observing Systems (EOS) are the MODIS and AIRS with high-spectral resolution. The MODIS is a new-generation remote-sensing optical instrument equipped with 36 spectral channels. Its horizontal resolutions at nadir are 250, 500, and 1 000 m, and its scanning width is 2 330 km (Liu and Yang[12]). The AIRS is an infrared detector with 2 378 channels that facilitate the simultaneous analysis of 2 378 samples. The AIRS observes the earth's surface by using a rotating scanning mirror. Its horizontal resolution at nadir is 13.5 km, and its vertical resolution is 1 km. One scanning line has a width of 1 650 km and is composed of 90 slots of the observational field of view, which includes 2 378 samples obtained via spectral sampling. A granule is composed of 135 scanning lines. The AIRS is capable of advanced infrared resensing and can provide detailed information on temperature and humidity profiles, sea surface temperature, surface emissivity, cloud fraction, cloud height, ozone content, and three-dimensional cloud distribution with high sensibility, accuracy, and precision; this information can be used to enhance the quality of numerical weather forecasts. Figure 2 shows the AIRS sounding image of a 1 000 cm^{-1} window channel obtained on August 11, 2004, when Typhoon Yunna approached the island of Taiwan and Mainland China.

In this study, the AIRS L1B radiance data, AQUA MOD03 geolocation file, and AQUA MOD35_L2 cloud products were downloaded from a NASA website. The sounding observation used to verify the retrieved temperature profiles was obtained from the Meteorological Satellite Integrated Application System 9210 Project (MICAPS). MICAPS (Zhang[13]) receives sounding data twice a day at 0800 CST (China Standard Time) and 2000 CST. We matched the temporal and spatial data with the retrieved profiles and verified them with respect to each other. The NCEP reanalysis products used in this research were downloaded from the NCEP center; the horizontal resolution is 1° in both the east-west and north-south directions. Its profiles contain 26 levels in the vertical section, including geopotential height, temperature, relative humidity, wind direction, wind speed, cloud liquid water, surface pressure, and ozone-mixing ratio. Since most domestic numerical weather-forecasting researchers use the NCEP reanalysis data to establish initial conditions for numerical models, we evaluated our retrievals with the NCEP profiles that temporally and spatially matched the retrieved profiles.

3 RETRIEVING ATMOSPHERIC PROFILES OF CLEAR SKY

To retrieve the atmospheric profiles under clear sky condition, the first step involves cloud detection of the AIRS pixel by matching it with the high-resolution MODIS cloud products. The second step involves retrieval of the atmospheric profiles using eigenvector regression and Newton's nonlinear physical iterative solution. This step includes preparation of training profile data, classification by brightness temperature and scanning angle, and generation of the background profile by eigenvector regression retrieval (Fig. 1).

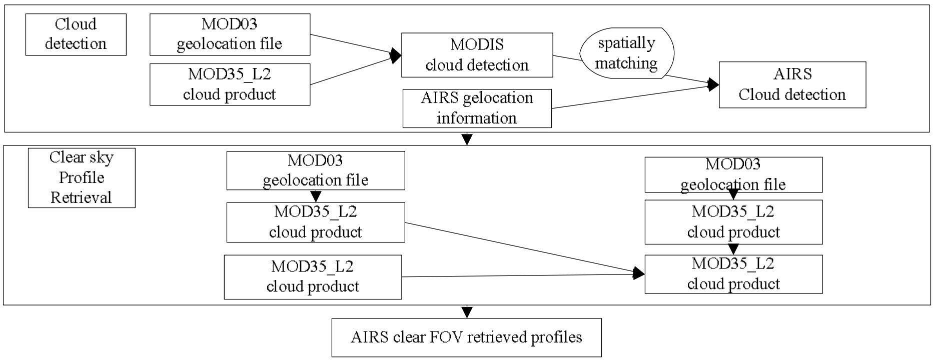

Fig. 1. Flowchart for retrieval of atmospheric sounding profiles of clear sky using AIRS

3.1 *Experiment design*

Cloud amount, cloud height, cloud characteristics, and the changes in these three parameters intensely influence the planetary albedo gradient and surficial exchange of energy. Furthermore, they influence the evolution of weather and climate systems. Cloud detection is extremely important for using satellite observations to study the reciprocity between cloud and synoptic systems. The results of cloud detection have a significant impact on the precision and accuracy of retrievals from satellite observation (Chevallier et al.[14]).

The observational precision of the AIRS with a high spectral resolution is sufficient to discern every CO_2 absorption line from the surface to a height of 40 km. However, the horizontal resolution of the AIRS is relatively too low (13.5 km at nadir), and consequently, there is no reliable cloud detection algorithm as to the AIRS observations. At the same time, the MODIS multispectrum and its high horizontal resolution (1 km at nadir) can clearly describe the three-dimensional structure of the clouds. Since MODIS and AIRS are located on the AQUA satellite, their scanning data are spatially and temporally consistent with each other. In this study, an AIRS with high spectral resolution is combined with the spatially and temporally matched MODIS cloud products. This combination is used for cloud detection and for retrieving the atmospheric profiles with good precision and high resolution.

First, we process the MODIS cloud product to obtain the cloud detection of MODIS pixels. AIRS cloud detection is objectively defined by the MODIS pixels that lie within the AIRS pixels. Thus, we can make sure whether an AIRS pixel is clear, partly clear, or completely cloudy. Figure 2 shows the AIRS sounding image of a 1 000 cm^{-1} window channel obtained on August 11, 2004, when Typhoon Yunna approached the island of Taiwan and Mainland China. Figure 2b indicates the cloud detection result of Typhoon Yunna approaching the island of Taiwan and mainland China, on August 11, 2004. Figures 2c & 2d show the retrieved surface temperature and surface pressure, respectively; Figures 2e & 2f show the corresponding surface temperature and surface pressure in the NCEP reanalysis, respectively. It can be observed that the retrieved atmospheric variables can reflect finer atmospheric structures than NCEP reanalysis data can.

3.2 *Application of principal component analysis*

Principal components (PCs) and eigenvector regression provide almost complete spectral information with little degradation, reduction in noise, temperature accuracy within tolerable limits, and water vapor retrieval. The technique is commonly used to reduce the dimensionality of a data set with a large number of interdependent variables.

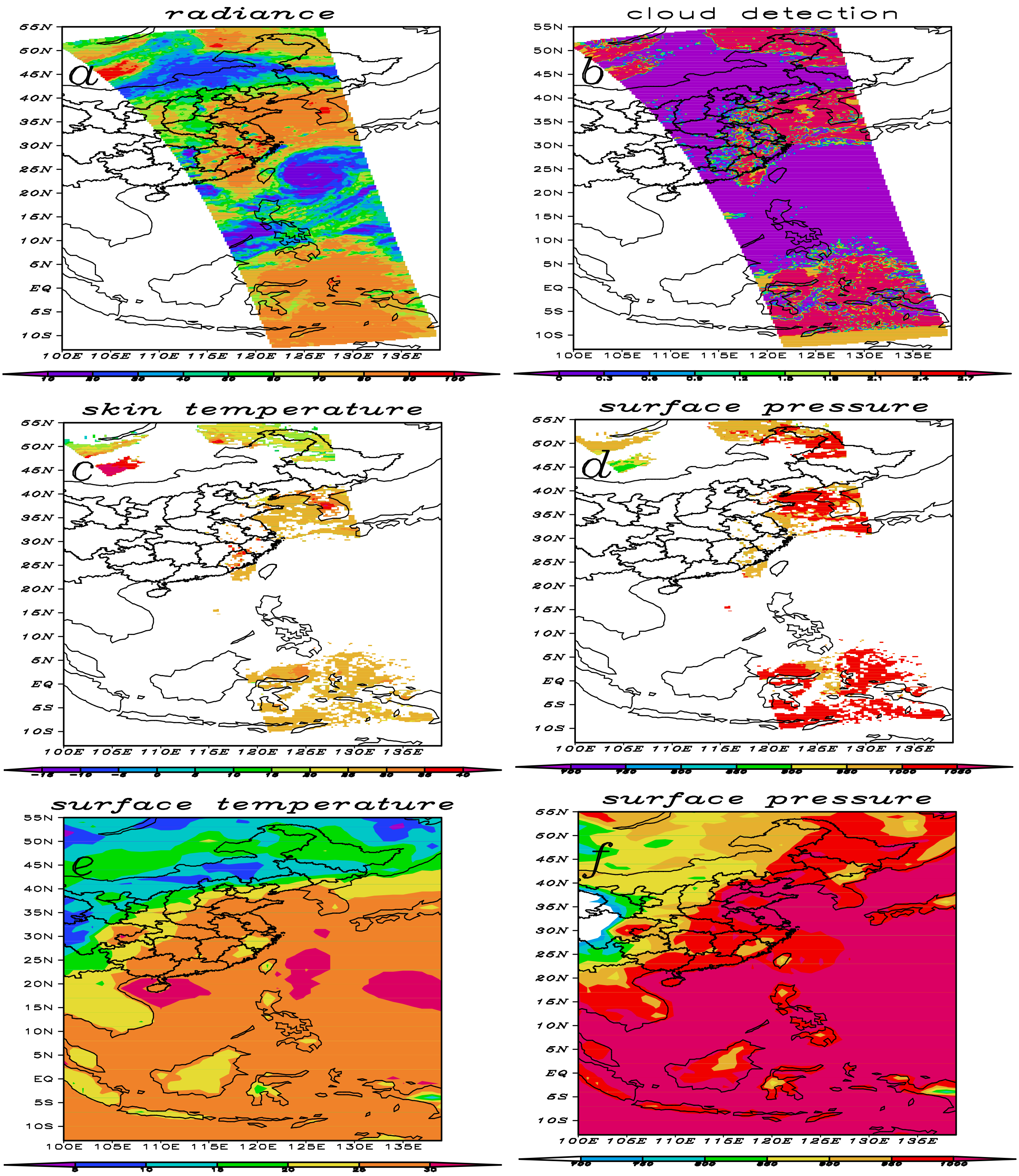

Fig. 2. AIRS Granule 050 051 052 from 0413 to 0517 CST August 11, 2004. (a) AIRS image of Typhoon Yunna (1 000 cm^{-1} channel) unit: $mW/m^2/cm^{-1}/sr$. (b) Cloud detection of Typhoon Yunna (0: absolutely cloudy; 1 and 2: partly cloudy; 3: absolutely clear; markings indicate the reliability). (c–d) The retrieved surface temperature (unit: °C) and the retrieved surface pressure (unit: hPa). (e–f) The NCEP surface temperature (unit: °C) and the NCEP surface pressure (unit: hPa).

An effective approach to retrieve atmospheric profiles is to adopt the statistical synthetic regression retrieval coefficient determined by training profiles and their simulated radiance values. In the practical retrieval process, the radiation values of carbon dioxide and water vapor window channels and the radiation values of other window channels are used to retrieve the temperature and humidity profiles. Such profiles then act as the first guess of Newton's nonlinear physical iterative solution. In the 1970s, Smith et al.[15] introduced a statistical regression algorithm. The retrieved variables in this study are composed of temperature profiles, relative humidity profiles, surface temperature and surface pressure. The profiles have 101 levels in the vertical direction. (Only levels greater than 100 hPa are listed in Table 1 because the top level of conventional sounding is 100 hPa).

Table 1. List of 57 levels greater than 100 hPa out of the 101 levels retrieved (pressure unit: hPa)

Level	1	2	3	4	5	6	7	8	9	10	11	12
Pressure	1 100.0	1 070.9	1 042.2	1 013.9	986.0	958.6	931.5	904.9	878.6	852.8	827.4	802.4
Level	13	14	15	16	17	18	19	20	21	22	23	24
Pressure	777.8	753.6	729.9	706.6	683.7	661.2	639.1	617.5	596.3	575.5	555.2	535.2
Level	25	26	27	28	29	30	31	32	33	34	35	36
Pressure	515.7	496.6	478.0	459.7	441.9	424.5	407.5	390.9	374.7	359.0	343.6	328.7
Level	37	38	39	40	41	42	43	44	45	46	47	48
Pressure	314.1	300.0	286.3	272.9	260.0	247.4	235.2	223.4	212.03	201.0	190.3	180.0
Level	49	50	51	52	53	54	55	56	57			
Pressure	170.1	160.5	151.3	142.4	133.9	125.7	117.8	110.2	103.0			

3.3 *Training data*

The original training data contain 12 000 globally distributed clear sky radiosonde profiles of temperature and humidity, along with observations of the surface temperature and pressure that comprise the global representative profiles of TIGR3 (TOVS Initial Guess Retrieval), NOAA88, and ECMWF. All profiles are extended from 1 100 to 0.005 hPa and then interpolated to the 101 levels. The radiative transfer calculation of the AIRS radiances is performed using the forward model, for each profile from the training data set, to produce a temperature-humidity profile-AIRS radiance pair. The synthetic regression coefficients are generated using the simulated radiances and the matching atmospheric profile. Then, according to the International Geosphere-Biosphere Programme (IGBP) ecological system, the training data is classified into 15 types.

3.4 *Classification on the basis of bright temperature*

To retrieve the profiles globally, the regression coefficients for different atmospheric and surface conditions in the algorithm were prepared. Training data were divided into six classes according to the brightness temperature at a wave number of 1 000 cm^{-1} (window channel). Table 2 lists the threshold values for each class of data. Each class of the brightness temperature observations corresponds to one set of regression coefficients. The purpose of brightness temperature classification is to improve the statistical regression accuracy and precision. Furthermore, we have overlapped each class by 10 K to avoid inaccurate regression results owing to an incorrect regression coefficient obtained by faulty classification.

Table 2. Scheme of classifying brightness temperature

Class	Training: BT at 1 000 cm^{-1}	Retrieval: BT at 1 000 cm^{-1}
1	BT ≤ 260	BT ≤ 255
2	250 < BT ≤ 270	255 < BT ≤ 265
3	260 < BT ≤ 280	265 < BT ≤ 275
4	270 < BT ≤ 290	275 < BT ≤ 285
5	280 < BT ≤ 300	285 < BT ≤ 295
6	290 < BT	295 < BT

3.5 *Forward model and classification on the basis of scanning angle*

The range of the AIRS scanning angle is from –49.5 to 49.5°. At nadir, the scanning angle is 0° and the field of view is circular; however, the field of view becomes elliptical as the scanning angle increases, and this ellipticity influences the observational radiation. Therefore, the classification based on the observed scanning angle was adopted along with the brightness temperature classification on the window channel. The values of the scanning angle ranging from 0 to 49.5° were divided into eleven types. In this study, the forward radiation transfer model (Strow et al.[16]) used for AIRS is the Stand-Alone Radiative Transfer Algorithm (SARTA, version 1.05). The AIRS utilizes the physical method to retrieve the atmospheric profiles; the results depend greatly on the speed and precision of the radiation transfer algorithm under a clear sky.

3.6 *Newton's nonlinear physical iterative solution*

If there is a satellite observer with K channels to watch the earth, we can define

$$Y=(y_1,y_2,\cdots,y_K)^T$$

where $y_i(i=1,2,\cdots,K)$ is the radiance (brightness temperature) of channel i. By minimizing the difference between synthetic observations and the regression forward model, we obtain the atmospheric temperature, water vapor, ozone profiles and the surface temperature if

$$J(X)=\left\|Y^m-Y(X)\right\|=\min$$

where Y^m is the actual AIRS measurement vector, X is the time and space colocated radiosonde profiles given by

$$X=(T_1,T_2,\cdots T_L,\ln q_1,\ln q_2,\cdots \ln q_L,\ln o_1,\ln o_2,\cdots,\ln o_L,T_s,\varepsilon_1,\varepsilon_2,\cdots,\varepsilon_{15},\cdots)$$

However, the retrieval problem is ill posed and additional information is needed to constrain the solution. Often this is accomplished by means of a first-guess profile obtained from a climate mean, a regression technique, and/or a collection of numerical forecast products. Then we can redefine $J(X)$ as

$$J(X)=\left\|Y^m-Y(X)\right\|+\gamma\left\|X-X^0\right\|$$

where X^0 is the first guess of X, γ is the Lagrange seed, $\|\cdot\|$ implies space in maths, we could apply Mahalanobis Space here

$$\left\|Y^m-Y(X)\right\|=[Y^m-Y(X)]^T E^{-1}[Y^m-Y(X)]$$

$$\left\|X-X^0\right\|=(X-X^0)^T B^{-1}(X-X^0)$$

where E is the covariance of the radiance observations, which include instrument noise and other sources of error, and B is the covariance of first-guess atmospheric profiles.

If we assume that $J'(X)=0$, then we can get the Newton's nonlinear physical iterative equation

$$\delta X_{n+1}=(F_n^T\cdot E^{-1}\cdot F_n+\gamma B^{-1})^{-1}\cdot F_n^T\cdot E^{-1}\cdot(\delta Y_n+F_n\cdot\delta X_n)$$

where F is the first derivative matrix of Y to X. When we minimize the difference $J(X)$, X_n will converge to a value X^* which will fit the observations and the profiles best.

4 ANALYSIS OF RETRIEVALS FOR CLEAR SKY

4.1 *Evaluation of retrieval for a single station*

The time observed in the AIRS granule 049 050 051 when Typhoon Yunna approached Taiwan Island and Mainland China ranged from 0413 to 0517 August 11, 2004. We have retrieved atmospheric profiles for the clear sky according to the aforementioned method and matched the retrievals with the 0000 UTC MICAPS radiosonde observations made on August 11, 2004. In all, 14 retrieved AIRS clear sky profiles match the radiosonde observations taken on August 11, 2004 temporally and spatially. The average observational time error of the retrieved AIRS clear sky profiles is 3 h and the space error is 90 km. In this study, we consider the results obtained from radiosonde observations to be the true values, and interpolate the retrieved AIRS profiles and NECP analysis profiles to the standard levels of the radiosonde observations and compute the statistical mean error and standard deviation between them.

Figure 3 shows that the retrieved thermometric error in all levels in the troposphere is less than 2.5 K; in this figure, black indicates the radiosonde observation value, red indicates the AIRS clear sky retrievals, and blue indicates the NCEP reanalysis profile. The red retrieved profile is closer to the black sounding profile (true value) than the blue NCEP reanalysis data; these retrievals are more advantageous than the NCEP reanalysis. Furthermore, the retrieved atmosphere profiles are clearer than the radiosonde observations due to linear hypotheses in the retrieval method. The horizontal resolution of the retrieved profile reaches 13.5 km (at nadir), and the vertical resolution is 101 layers. The average error in the retrieval is approximately 2.5 *K*; hence, the precision required for operational applications and numerical model applications is attained. The profiles can be used to improve the initial field of numerical prediction, thereby improving the accuracy of numerical prediction. We can also directly analyze typhoonic mesoscale structures using these profiles because of their high-resolution feature.

4.2 *Evaluation of retrieval for several stations*

To further investigate the retrieved temperature, humidity profiles, and other variables, we proceed with our retrieval procedure and evaluation (See Table 3) of ascending AIRS observation granules covering Middle- and East-China from August 1, 2004 to August 11, 2004, the statistics of the number of matched stations and the standard deviation and standard error between them. It is observed that the mean deviation between the retrievals and the sounding observational profiles of more than 400 levels for 122 stations in eight days is 2.397 K, while the mean deviation in the NCEP reanalysis is 8.952 K, which is four times that in the AIRS retrievals. Furthermore, the horizontal resolution of the retrievals is approximately 13.5 km (at nadir), whereas the horizontal resolution of the NCEP reanalysis is 1° (approximately 100 km at middle-high latitude). The horizontal and vertical resolutions and the precision of the retrieved profiles are better than those of the NCEP reanalysis data.

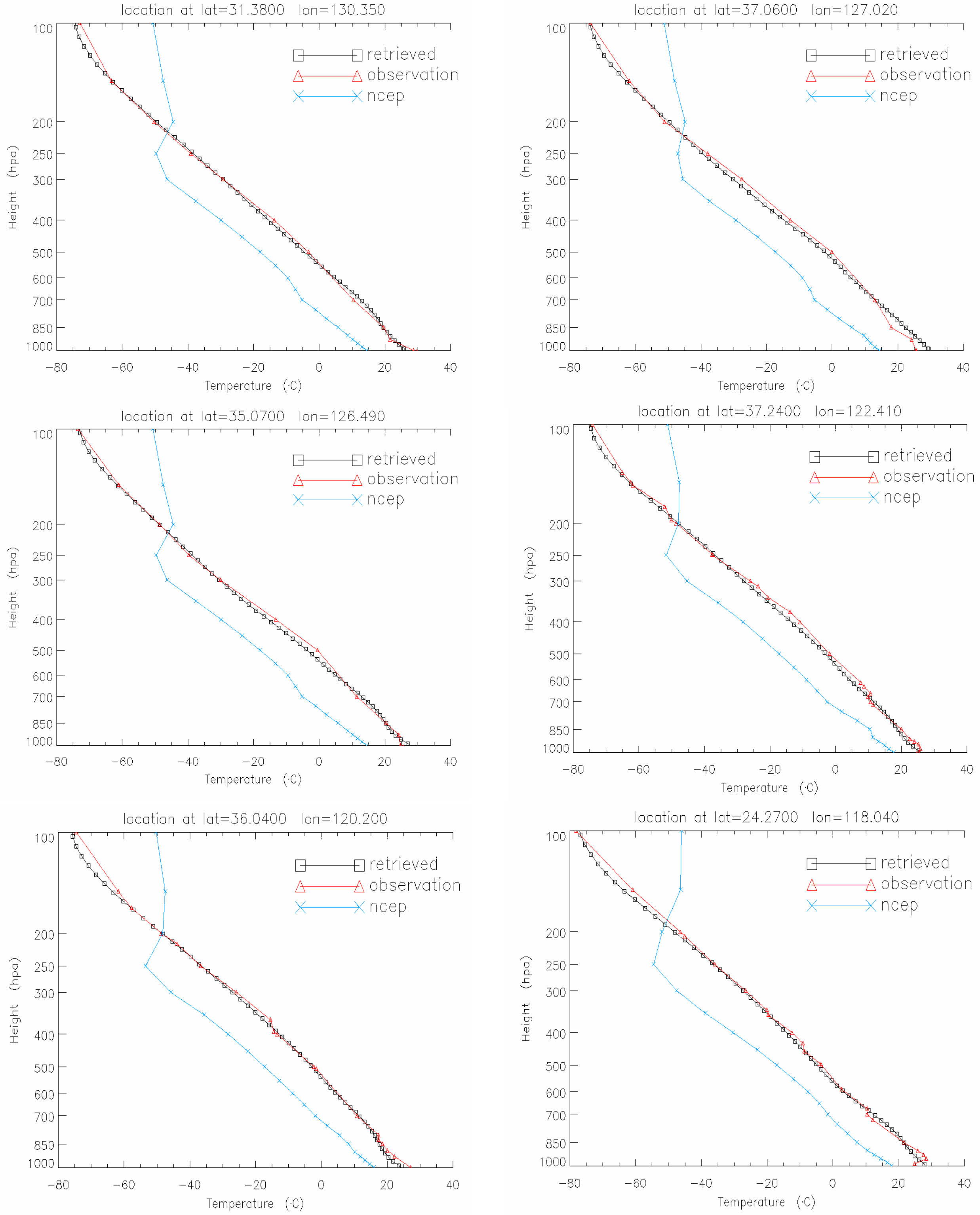

Fig. 3. Comparison between the retrieved atmospheric sounding temperature profiles of clear sky obtained using infrared hyperspectral measurements AIRS (granule 050 051 052) and the sounding observations. Further, comparison of the average deviation and the standard deviation between the NCEP profile and the sounding observation obtained on August 11, 2004, is shown (black: station observations; red: retrieved profile; and blue: NCEP analysis profile; unit: °C).

Table 3. Average deviation and standard deviation between the retrieved atmospheric sounding profile using AIRS infrared hyperspectral measurements under clear sky and the sounding observation. The average deviation and standard deviation between the NCEP profile and the sounding observation from August 1–8, 2004 (Unit: K)

Date (2004)	Number of retrieved profiles matched with station	Average deviation between retrieved profiles and observation	Average deviation between NCEP and observation	Standard deviation between retrievals and observation	Standard deviation between NCEP and observation
1 AUG	14	2.39745	8.95189	3.93942	14.23830
2 AUG	19	1.94286	10.19182	3.30896	16.28426
3 AUG	7	2.25756	11.10016	3.84442	16.27623
4 AUG	18	2.30215	7.53835	4.07072	13.32577
5 AUG	9	2.13957	9.09042	4.01348	14.26361
6 AUG	21	2.27106	10.84216	4.28276	18.63050
7 AUG	10	2.52134	6.27062	4.87446	10.56610
8 AUG	24	2.35647	8.91801	4.24337	14.38242
Average	15.25	2.27356	9.11293	4.07220	14.7459

5 CONCLUSION AND SUMMARY

By employing the principal eigenvector component analysis/retrieving algorithm, we could rapidly and accurately retrieve the atmospheric temperature and ozone profiles along with the surface pressure, surface temperature, and surficial emissivity. The regression coefficient is obtained from substantive sample profiles and their simulated radiation values. Moreover, the simulated value is compressed by employing an eigenvector that will increase the retrieving efficiency and stability and simultaneously decrease the influence of random noise. In order to make the algorithm globally applicable, training sample data includes different types of global representative atmospheric profiles in different atmospheric states and under different surficial conditions. The retrievals obtained by this method are in good agreement with the atmospheric sounding observational distribution; these retrievals even reflect very fine atmospheric structure due to their high infrared hyperspectral resolution (high vertical space resolution). However, in this study, we simply retrieved the profiles and evaluated them with NCEP data and sounding observations. These profiles can be used to improve numerical models, and the effect of these profiles on the initial conditions of the model and the accuracy of its prediction can be examined.

Acknowledgements: We sincerely thank Allen Huang of American Wisconsin University for sharing the programs at ftp://ftp.wisc.ssec.edu. Further, we are grateful for being allowed to obtain the AIRS L1B data, MOD03 geolocation file, and MOD35 cloud product from www.gsfc.nasa.com

REFERENCES:

[1] ANDERSSON E, PAILLEUX J. Use of cloud-cleared radiance in three/four-dimensional variational data assimilation [J]. Quart. J. Royal. Meteor. Soc., 1994, 120: 627-653.

[2] MILIJA Z. Regional Four-Dimensional Variational Data Assimilation in a Quasi-Operational Vapor, and Cloud Water Profiles from Advanced Microwave Sounding Unit (AMSU)[J]. IEEE Transaction on Geoscience and Remote Sensing, 1993, 12: 2 396-2 408.

[3] GAO Shou-ting, ZHOU Yu-shu, LEI Ting, et al. Analyses of hot and humid weather in Beijing city in summer and its dynamical identification [J]. Science in China (Ser. D Earth Sci.), 2005, 48(Supp. II): 128-137.

[4] GAO Shou-ting, LI Xiao-fan, TAO Wei-kuo, et al. Convective and moist vorticity vectors associated with tropical oceanic convection: A three-dimensional cloud-resolving model simulation [J]. J. Geophys. Res., 2007, 112, D01105.

[5] GUAN Li. A study on infrared hyperspectral measurements and its applications on cloud detection, cloud-clearing and atmospheric sounding profile [D]. Theses for Doctoral Degree, Nanjing: Nanjing Univ. Info. Sci. & Technol., 2005: 11-40.

[6] GUAN Li, HUANG H L, LI Jun. A pilot study of retrieving atmospheric profiles using EOS/AIRS observations [J]. Acta Meteor. Sinica, 2005, 19: 112-120.

[7] CUI Cai-xia, YANG Qing, YANG Lian-mei. The computation of surface temperature of Taklamagan desert using MODIS data [J]. China Desert, 2003, 23: 596-599.

[8] LI Hui. Retrieving of ozone content using satellite observation data [D]. Theses for Master Degree, Beijing:

Chinese Academy of Meteorological Science, 2003: 27-39.
[9] HUANG H L, ANTINELLI P. Application of principal component analysis to high resolution infrared measurement compression and retrieval [J]. J. Appl. Meteor., 2001, 40: 365-388.
[10] HUANG H L, SMITH W L. Apperception of clouds in AIRS data, ECMWF Workshop on Assimilation of high spectral resolution sounders in NWP [C]. Shinfield Park: ECMWF, 2004, 155-169.
[11] XU Ying-long, GAO Shuan-zhu, LIU Zhen-kun. Analysis on the maintaining of typhoon Yunna [J]. Mon. Meteor., 2005, 31: 31-36.
[12] LIU Yu-jie, YANG Zhong-dong. Principle and Arithmetic of Processing MODIS Resensing Information [M]. Beijing: Science Press, 2001: 1-4.
[13] ZHANG Guo-cai. Training material of meteorological satellite broadcasting system [M]. Beijing: Meteorological Press, 2001: 1-204.
[14] CHEVALLIER F, BAUER P J, MAHFOUF F, et al. Variational retrieval of cloud profile from ATOVS observation [J]. Quart. J. Roy. Meteor. Soc., 2002, 128: 2 511-2 525.
[15] SMITH W L, WOOLF H M, JACOB W J, et al. A regression method for obtaining real-time temperature and geopotential height profiles from satellite spectrometer measurements and its application to Nimbus 3 "SIRS" observation [J]. Mon. Wea. Rev., 1970, 98: 582-603.
[16] STROW L L, HANON S E, MOTTELER H E. An Overview of the AIRS Radiative Transfer Model [J]. IEEE Trans. Geosci. Remote Sensing, 2003, 41: 303-313.

Citation: HUANG Bing, LIU Jian-wen, BAI Jie et al. Retrieving atmospheric sounding profiles around Typhoon Yunna using infrared hyperspectral measurements AIRS. *J. Trop. Meteor.*, 2010, 16(3): 201-209.